Technical Paper

BR-1857

Effects of Moisture on Char Burnout During Warm-Recycle Oxy-Coal Combustion

Authors:
S. Hu
D. Zeng
A. N. Sayre
H. Sarv

Babcock & Wilcox
Power Generation Group, Inc.
Barberton, Ohio, U.S.A.

B&W babcock & wilcox power generation group

Effects of Moisture on Char Burnout During Warm-Recycle Oxy-Coal Combustion

S. Hu
D. Zeng
A. N. Sayre
H. Sarv
Babcock & Wilcox Power Generation Group, Inc.
Barberton, Ohio, U.S.A.

Abstract

Oxy-coal combustion is a viable technology for curtailing greenhouse gas emissions from coal-fired power plants. It is a process of burning coal with flue gas diluted oxygen. Depending on where the recycled flue gas (RFG) stream is extracted, different combustion characteristics can be expected. "Cold-recycle" and "warm-recycle" modes of oxy-coal combustion are two ways of operating a power plant largely dictated by the fuel sulfur content. Under the warm-recycle condition, the flue gas moisture is not removed from the secondary oxidant stream, and the overall moisture content inside the boiler under steady-state operating condition could reach 35 vol%. The effect of the elevated moisture and CO_2 levels on char burnout is the main subject of this study.

Previously, char burnout was studied under cold-recycle oxy-coal combustion and air-firing conditions. It was concluded that char-CO_2 gasification reactions can play an important role in char burnout. This effect is dependent on both coal rank and combustion condition. Continuing investigation began with the study of the effect of H_2O-rich gas on char burnout under warm-recycle oxy-combustion conditions using a western sub-bituminous coal as compared to the cold-recycle oxy- and air-firing conditions. All three conditions were generated on a flat flame burner (FFB) facility in which gaseous fuel and oxidizer mix and burn rapidly above its surface to produce a high temperature, one-dimensional flame zone. By adjusting the gaseous feed (fuel type, relative flow rate and inert dilution ratio), desired flame environment (temperature, $O_2/CO_2/H_2O$ levels, etc.) can be generated. The pulverized sub-bituminous coal and its respective char (derived under a hot and inert atmosphere) were fed separately into the flame zone with 4 vol% oxygen that simulated post-flame boiler environment. Char samples at different residence times were collected and their extent of burnout was determined using the ash tracer technique. An optical fiber based two-color pyrometer was used to simultaneously acquire single particle surface temperature and velocity data. Experimental results demonstrated that high CO_2 and H_2O levels under oxy-firing conditions affect char burnout in two ways. On one hand, the char-CO_2 and char-H_2O gasification reactions can enhance burnout through direct consumption of char. On the other hand, the endothermic nature of these reactions can lower the particle surface temperature and hence decrease the char oxidation rate, which in turn leads to lower char conversion. The dominance of either effect is dependent on the coal type and the firing conditions (gas temperature, species concentrations, etc.). Char burnout for the sub-bituminous coal in the low-moisture, cold-recycle condition was higher relative to air-firing operation due to the dominance of char gasification by CO_2. In contrast, char burnout under warm-recycle oxy-combustion was similar to that of air-firing, indicating that the anticipated char gasification enhancement was equally negated by a cooler particle temperature.

The work is accompanied by modeling activities where the char oxidation sub-model in Babcock & Wilcox Power Generation Group, Inc.'s (B&W PGG) COMO^{SM} CFD code is evaluated under the test conditions. Both mass release and particle temperature data are predicted using Field's char oxidation sub-model with gasification by both CO_2 and H_2O considered. New kinetic rate parameters are derived from the experimental results.

Nomenclature

BFB Bubbling Fluidized Bed
CBK Char Burnout Kinetic Model
CFD Computational Fluid Dynamics
COMO Combustion Model (B&W PGG's proprietary
         CFD code)
CPD Chemical Percolation Devolatilization
DAF Dry Ash Free Basis
ESP Electrostatic Precipitator
FFB Flat Flame Burner
PC Pulverized Coal
PGSL Probabilistic Global Search Lausanne
PRB Powder River Basin
RFG Recycled Flue Gas
vol% Percentage by Volume

Introduction

Oxy-coal combustion is a viable technology for curtailing greenhouse gas emissions from coal-fired power plants. Since combustion of fuel with pure oxygen results in very high flame temperatures, flue gas recycling is applied to control the temperature and provide adequate gas flow over the heat absorption surfaces. Depending on where the recycled flue gas (RFG) stream is extracted, different combustion characteristics can be expected. "Cold-recycle" and "warm-recycle" modes of oxy-coal combustion are two ways of operating a plant largely dictated by the fuel sulfur content. Under the cold-recycle condition, the RFG is taken after the wet flue gas desulfurization (WFGD) scrubber where the moisture level is only a few percent by volume. Under the warm-recycle condition, the RFG is extracted after the air heater and before the particulate capture system. Since the flue gas moisture is not removed from the secondary oxidant stream, the overall moisture content inside the boiler under steady-state warm-recycle operation could reach 35 vol%. Detailed knowledge of the effects of H_2O and CO_2 on char reactivity is important for accurate determination of char burnout and implementation in predictive combustion models.

A recent study [1] has shown that even though the oxy-coal combustion process is reasonably well understood, certain areas such as flame stability, radiative heat transfer, effects of H_2O, and corrosion issues related to SO_2/SO_3 still deserve further in-depth investigation. Another review [2] puts similar focus on oxy-coal combustion research. Many research groups [3-11] have identified the importance of char gasification by CO_2 under oxy-coal combustion. However, there has been no study reporting the effects of high levels of H_2O, an inherent characteristic of warm-recycle oxy-coal combustion.

Similar to CO_2, high concentration of H_2O is likely to affect char oxidation through enhanced char gasification reactions, which in turn results in higher char burnout. However, due to the endothermic nature of the gasification reactions, the particle surface temperature will decrease, which in turn decreases oxidation rate and results in lower char burnout. These two effects compete with each other and their relative importance is likely dependent on coal type and local flame conditions such as temperature and oxygen level. The relative importance of each effect on char burnout cannot be obtained from char burnout data alone. Particle surface temperature measurement has to complement the burnout data to obtain a good understanding.

Two-color pyrometer has been used by several research groups to simultaneously obtain temperature, particle size and velocity data [12-18]. Temperature was determined based on the ratio of signal from two different wavelength bands by applying the radiation law. Particle velocity was inferred from a time-of-flight method. An optical fiber-based, two-color pyrometer designed and fabricated from earlier studies is used here to obtain single particle surface temperature information.

Most of the earlier studies have focused on char combustion at relatively high oxygen levels. However, in staged combustion, a char particle spends a significant amount of its lifetime in a reducing environment with little or no O_2 but abundant CO_2 and H_2O. Char gasification at such conditions is enhanced by elevated concentrations of CO_2 and H_2O under oxy-combustion. In this study, the oxygen level in the FFB flame was set to match typical boiler conditions. To isolate the char oxidation/gasification reactions during the experiments, char samples prepared by driving volatiles off its parent coal in an inert atmosphere are tested under the same conditions. Test data from both coal and char samples are obtained.

In this work, we investigated the effects of high concentrations of CO_2 and/or H_2O on char burnout and obtained a set of mass loss and particle surface temperature data for a low sulfur sub-bituminous coal under representative air-firing, cold- and warm-recycle oxy-combustion conditions. In addition, we also validated and optimized existing char oxidation sub-model in B&W PGG's proprietary COMO™ CFD program. New kinetic rates were deduced and optimized from the experimental data obtained from this work.

Experimental setup

Flat flame burner

A schematic of the experimental setup of the FFB is shown in Figure 1. The burner produces a high temperature zone utilizing gas combustion. A $CO-H_2-N_2$ or $CO-H_2-CO_2$ mixture is used as fuel and an O_2-N_2 or O_2-CO_2 mixture is used as oxidizer. Fuel supply is directed to the burner surface through hypodermic tubes and oxidizing gas flows through the honeycomb to mix with the fuel at the burner surface. A central 1.33 mm ID tube is installed along the flat flame burner centerline for coal particle injection. A removable quartz viewing tower shields the flame from air entrainment. The solid particle feeder is similar to the one used by Ma [19]. It consists of a stepper-motor-driven
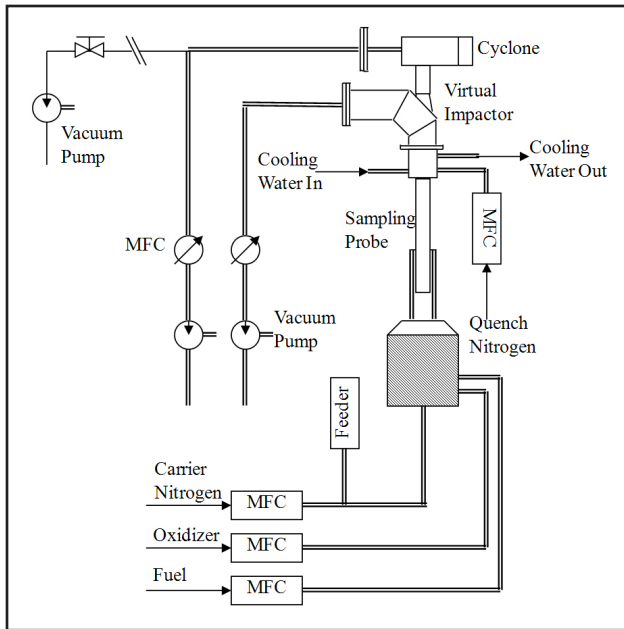
Fig. 1 The flat flame burner system.

syringe, a sealed gas funnel, and particle conveying tubes. A computer-controlled step motor translates the plunger at a predefined speed which pushes the coal particles into the vertically mounted funnel from a side port. Carrier gas flow enters from the top of the funnel to transport coal or char particles into the central injection tube.

A picture of the FFB flame with simultaneous pulverized coal injection is shown in Figure 2. The blue colored radiation towards the surface of the burner is from $CO/H_2/O_2$ combustion. The bright yellow streak in the middle of the picture is a result of coal volatile and char combustion. The collection probe is located above the pictured region.

Two-color pyrometer

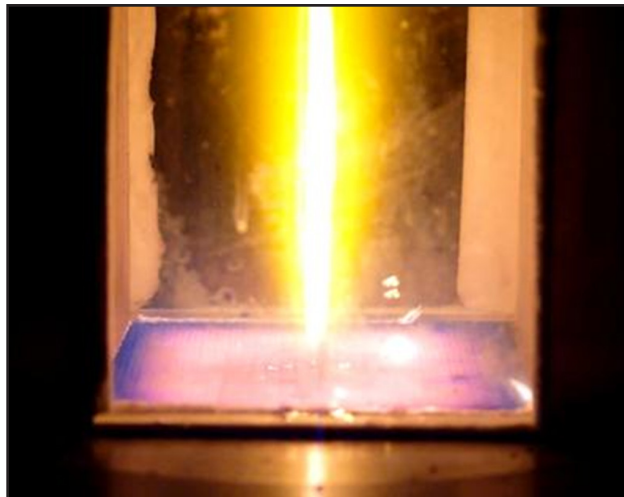The setup of the two-color pyrometer system is shown in Figure 3. Particle-emitted light is collected by a plano-convex lens (100 mm f.l.) and focused into a fiber bundle which contains two 1.5 mm silica fibers and four 600 μm fibers. The arrangement of the fibers is shown in the inset of Figure 3. The separation distance of the two big fibers is L=3 mm from axis to axis. Light from the top primary fiber provides measurement for particle temperature and size, as well as the start time for the time-of-flight velocity measurement. The reference fibers ensure the particle is fully exposed to the primary fibers. Light from the top primary fiber is collimated and split by a longpass filter (1050 nm cutoff). A Si photodiode (400 to 1100 nm) with built-in preamplifier is used to detect the light in the short wavelength range, and an InGaAs detector (700 to 1700 nm) with an external amplifier is used to detect the light in the long wavelength range. The light from the bottom primary fiber and four reference fibers is detected by two Si photodiodes with built-in preamplifiers, respectively. More details about the device can be found in an earlier publication [11].

Test conditions

The burner is operated at a nominal peak flame temperature of 1800 K across the different test conditions. In all of the tests, the excess oxygen level is kept constant at 4 vol%. The PRB coal (western sub-bituminous) and its derived char are used in this study. Its approximate and ultimate analysis is summarized in Table 1. To generate the char samples used for testing, the pulverized coal, 106 to 125 μm, is pyrolyzed in a bench-scale BFB reactor at 973 K in nitrogen gas for ~15 minutes.

Three firing conditions, air-firing, cold- and warm-recycle oxy-firing, are simulated in this study on the FFB. The air-firing is simulated by CO-H_2-O_2 combustion using N_2 as a diluent. H_2 is used only in very small amounts to stabilize the flame. The moisture in the product gas is approximately 1 vol%. The cold-recycle oxy-firing is simulated by replacing N_2 with CO_2. The warm-recycle oxy-firing condition is achieved by increasing the H_2 content in the fuel supply while maintaining the same peak flame temperature. The moisture level under this condition is 35 vol%. The temperature and oxygen and moisture concentration profiles measured as a function of reaction distance are shown in Figure 4 and Figure 5.
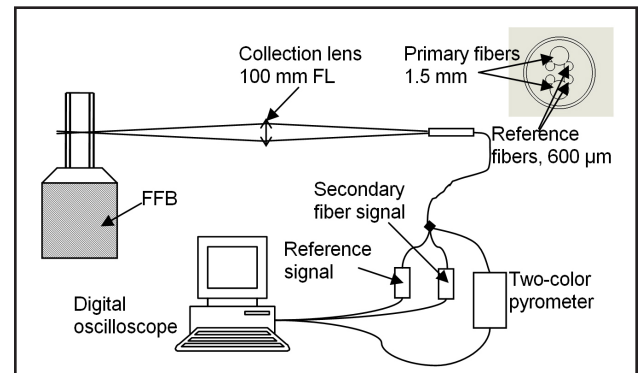

Fig. 2 Image of a representative FFB flame.

Fig. 3 Setup of the two-color pyrometer system.

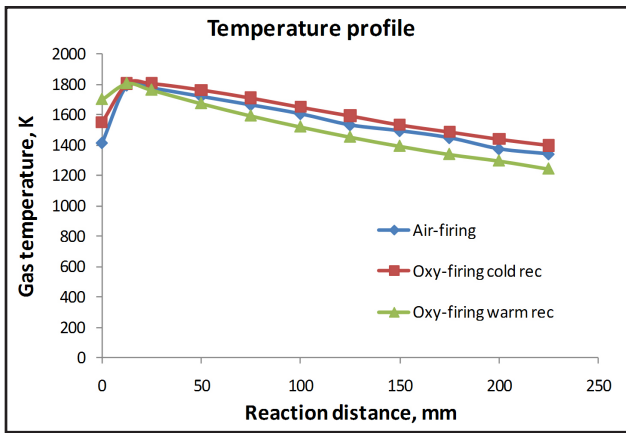**Fig. 4** Temperature profiles for the three test conditions.

Fig. 5 Species concentration profiles for the three test conditions.

The tests carried out in this study are summarized in Table 2. Both char sample collection and particle surface temperature measurement using the two-color pyrometer are carried out at 4 or 5 reaction distances under each flame condition for both coal and char feeding. Mass release is determined using ash as a tracer.

Results and discussion

Experimental results

As mentioned earlier, both PRB coal and char are injected to the FFB respectively. An important difference can be observed between the combustion of these two different types of particles. Due to the lack of volatile flame in the case of char injection, the luminescence signal from the particle combustion increases monotonically with reaction distance. However, in the case of coal feeding, a distinct volatile flame always precedes the slower and less intense char combustion.
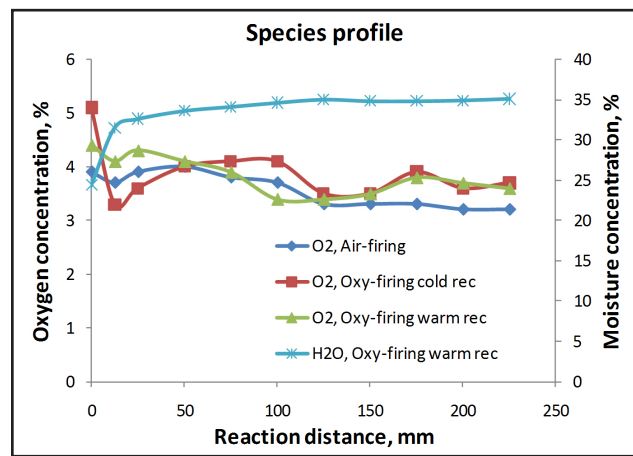
Mass release

Differences in total mass release are observed among three firing conditions when PRB coal is injected (Figure 6 – left). Mass release under cold-recycle condition is the highest, followed by air-firing and then warm-recycle. In the case of PRB char injection, cold-recycle still gives the highest mass release (Figure 6 – right). However, the mass release under air-firing and warm-recycle is similar. Contrary to expectation that gasification of char with CO_2 or H_2O results in higher mass release, a lower mass release is observed for both coal and char under warm-recycle conditions. The answer to this apparent anomaly will emerge from a later discussion.

Elemental mass releases of the char samples including C, H, N, S, and O are also measured. The results for both PRB coal and char under various test conditions are shown in Figure 7. Common among the coal and char results, the mass release rates of both hydrogen and oxygen are higher than the total mass release rate (designated by the diagonal dashed line in the figure). The release rate of nitrogen is

Table 1
Fuel Analysis (as received basis)

Sample type	Moisture, %	Volatile Matt., %	Fixed C, %	Ash, %	C, %	H, %	N, %	S, %	O, %
PRB Coal	4.63	40.42	48.89	6.05	67.63	4.92	0.93	0.29	19.9
PRB Char	3.25	--	--	8.83	77.47	1.75	0.89	0.25	7.58

Table 2
Test Matrix

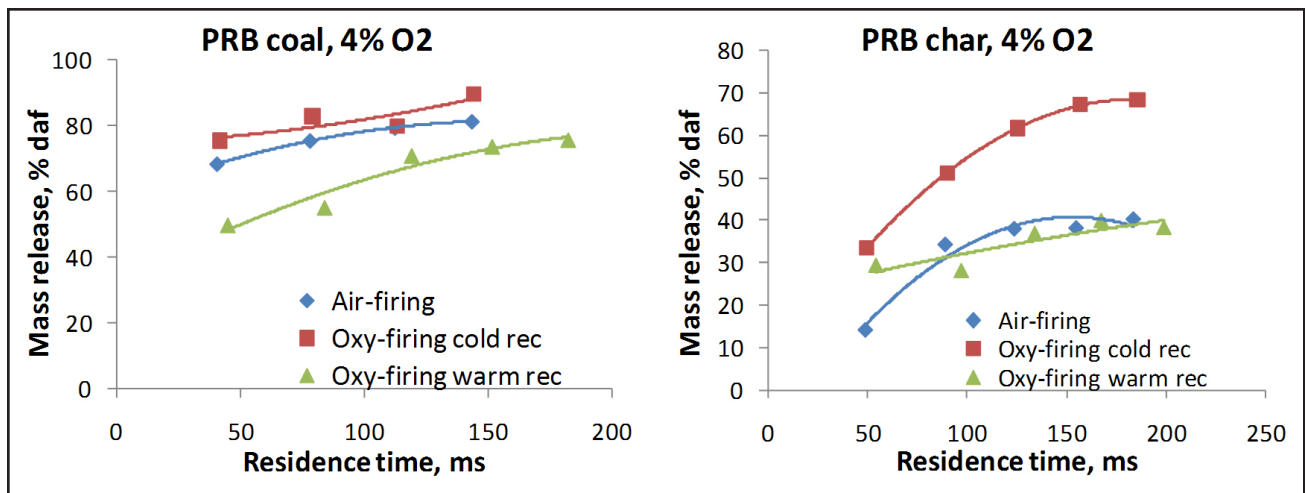| FFB Test Condition		Residence Distance, mm	T, K	Mass Release	Particle Temperature
Air-firing	4% O_2 in N_2	50,100, 150, 200, 250	1800	Both coal and char	Both coal and char
Cold-recycle oxy-combustion	4% O_2 in CO_2				
Warm-recycle oxy-combustion	4% O_2 in 35% H_2O + bal. CO_2				

Fig. 6 Mass release of PRB coal and char under three simulated firing conditions.

less than the total, while the carbon release rate is in the vicinity of the total. Observed from coal feeding data, sulfur release is much lower in both the air-firing and cold-recycle conditions than that of carbon, but becomes similar to that of carbon under the warm-recycle condition. This indicates a different sulfur release mechanism under the influence of moisture that warrants further study.

Particle temperature

Thousands of single particle data are recorded for each test condition using the two-color pyrometer. The data reduction program automatically rejects data that have a high relative reference fiber signal [11]. In general, under each test condition at a single reaction distance, the final data set contains data from 300 to 400 individual particles. The measured single particle surface temperatures are number-averaged and presented hereafter. The two-fiber design of the two-color pyrometer also enables particle velocity measurement using a time-of-flight method. During data reduction, the averaged velocity data are plotted against reaction distance. A polynomial curve-fitting and extrapolation towards the burner surface gives the velocity at locations before particle ignition where no luminescence signal is detectable. Integration of the fitted curve produces the correlation between the residence time and reaction distance.

Shown in Figure 8 are the average particle temperature data at different residence times for both PRB coal and char under the three simulated firing conditions. The particle temperature decreases with increasing residence time due to the decrease in the gas temperature because of the heat loss, but it is generally 100 to 200 degrees higher than the ambient gas temperature.

In both coal and char injection cases, the particle temperature under air-firing condition is the highest, followed by that of the cold-recycle oxy-firing. Warm-recycle oxy-firing produces the lowest particle temperature. The difference in particle temperatures among these environments should be attributed to the endothermic gasification reactions. The

reduced particle surface temperature is in turn affecting the rate of oxidation reactions which reduces mass release. In the case of cold-recycle oxy-firing, the reduction in oxidation rate due to reduced surface temperature does not out-pace the increased mass release rate due to CO_2 gasification. As a result, cold-recycle enhances mass release (Figure 8). However, in the case of warm-recycle oxy-firing, the opposite is true, i.e., the reduction in oxidation rate due to decrease in particle surface temperature because of the gasification reactions out-paces the increased mass release due to the combined char gasification with CO_2 and H_2O. As a result, warm-recycle hinders mass release (Figure 8).

However, it is erroneous to conclude that warm-recycle oxy-combustion results in lower mass release. Shown in Figure 9 are the Arrhenius plots of reaction rate as a function of a measured particle surface temperature under three firing conditions. The reaction rate is normalized against the initial particle weight on a DAF basis. For both coal and char cases, at a given temperature, the reaction rate under warm-recycle oxy-firing condition is the highest, followed by cold-recycle and then by air-firing. This is not surprising because in the oxy-firing cases, the normalized reaction rate plotted in Figure 9 includes contributions from gasification reactions by CO_2 and water. The implication, however, is that under warm-recycle oxy-combustion, the boiler needs to be operated at an oxygen level higher than air-firing to achieve similar carbon burn out. In order for the CFD model to produce an accurate prediction, the char oxidation sub-models need to consider the effects of the gasification reactions. Our attempt toward sub-model improvement is presented in the next section.

Sub-model improvement

A single-particle model is used to simulate the experimental conditions in this work. In this model, the particle is treated as stationary by setting its velocity to zero. Selected variables can be entered in the form of polynomial profiles as a function of reaction distance. Actual profiles of gas
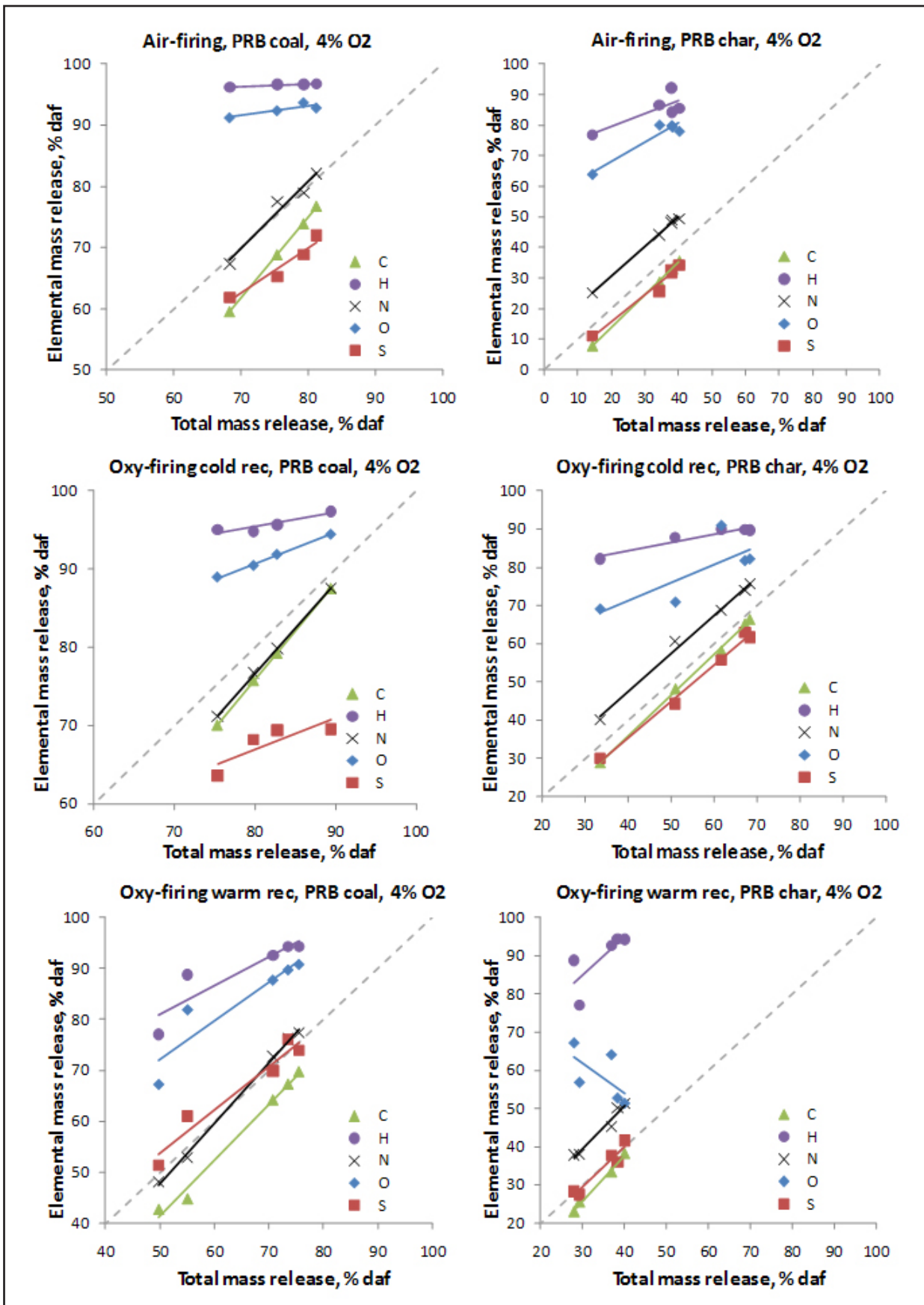
Fig. 7 Elemental mass release of PRB coal and char under three simulated firing conditions (left column: PRB coal; right column: PRB char).
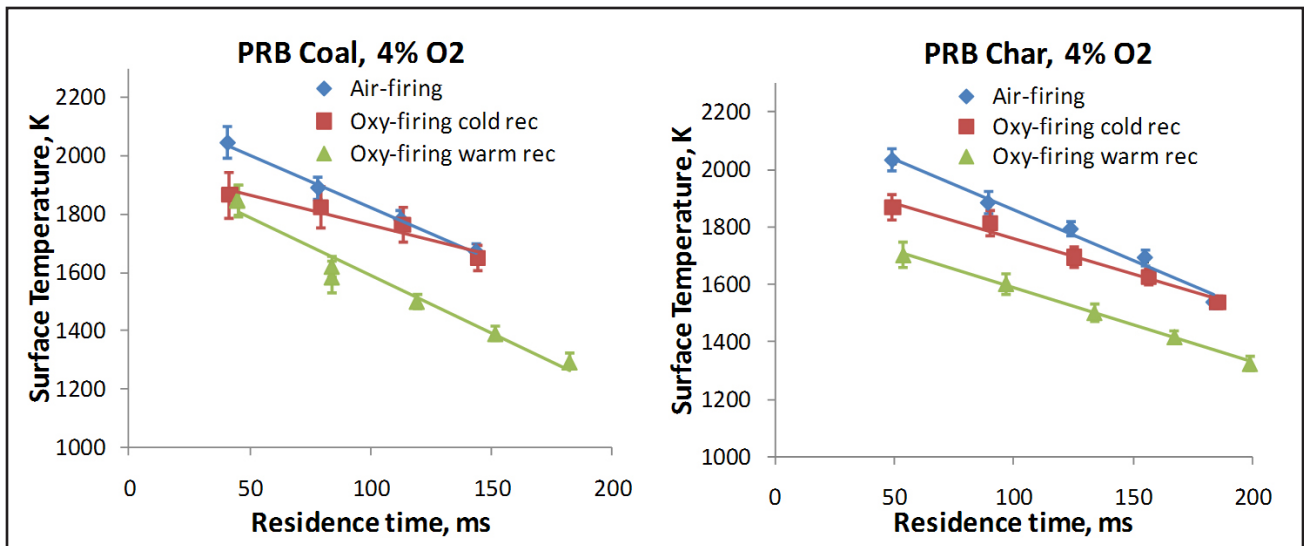
Fig. 8 Particle surface temperature of PRB coal and char under three simulated firing conditions (left: PRB coal; right: PRB char)

temperature, particle velocity, and oxygen and moisture concentrations are provided as model inputs. In the case of coal feeding (as compared to char feeding), the devolatilization step is modeled using the CPD sub-model [20]. Field's char oxidation sub-model [21], including gasification reactions by CO_2 and H_2O, is used to simulate char mass release and particle surface temperatures. There are four Arrhenius-type rate expressions that need to be considered in Field's model. They are associated with the following:

1. Char gasification with carbon dioxide:
   $$C(s) + CO_2 \rightarrow 2\,CO$$
2. Char gasification with water vapor:
   $$C(s) + H_2O \rightarrow CO + H_2$$
3. Char oxidation:
   $$C(s) + \tfrac{1}{2}\,O_2 \rightarrow CO$$
4. CO oxidation on char surface:
   $$CO/CO_2 = A_4\,exp(-E_4/(RT))$$

The pre-exponential factor and activation energy for each reaction are designated by A and E respectively with subscript 1 through 4 referring to each reaction. The gasification and oxidation reactions are treated as unity-order and half-order in the model respectively. Expression 4 is a pseudo expression to quantify the formation of CO and CO_2 on the surface of char. In this study, we utilize the existing model structure and performed rate parameter optimization using a routine based on the PGSL method [22]. There are a total of eight parameters that can be optimized (two for each Arrhenius expression).

The optimization subroutine seeks pre-exponential factor and activation energy values that give a minimal value of the error function. The error function is defined as:

$$\chi^2 = \sum_i \left[\left(\frac{T_{P,m} - T_{P,c}}{T_{P,m}} \right)^2 + \left(MR_m - MR_c \right)^2 \right] \quad (1)$$
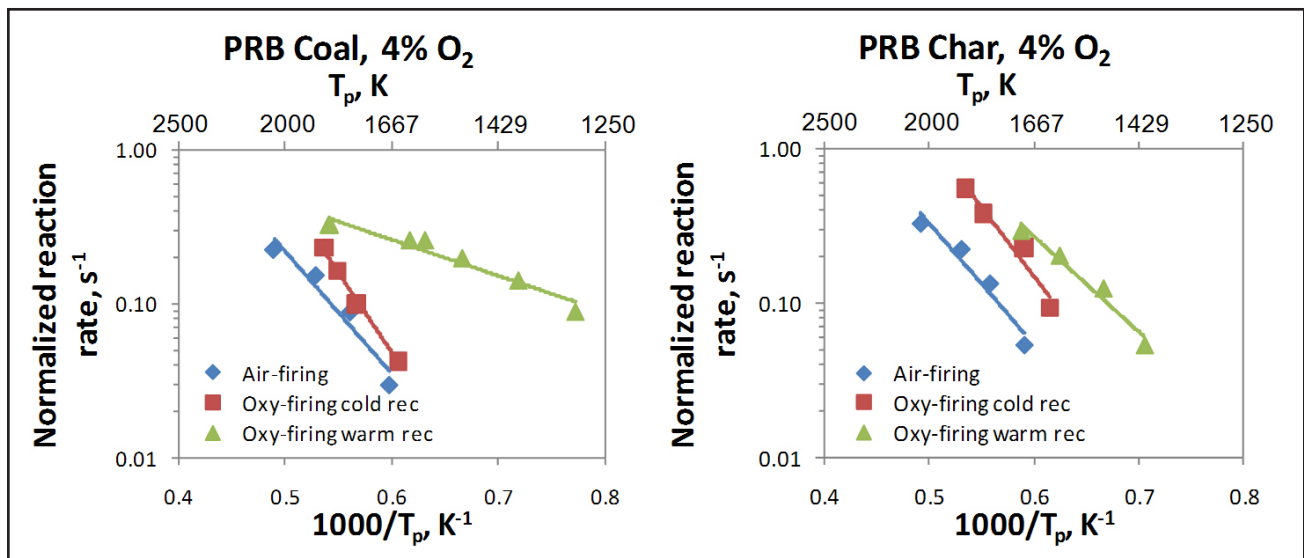

Fig. 9 Arrhenius plot of normalized reaction rate as function of temperature under three simulated firing conditions (left: PRB coal; right: PRB char).

where T and MR refer to temperature and mass release respectively. Subscripts p, m and c refer to particle, measured and calculated respectively. The error function puts equal weight factor to the temperature and the mass release data. Summation over subscript i refers to all of the test cases in this study (different firing condition and reaction distances).

The char oxidation kinetic and product ratio parameters were then optimized independently using published data from Sandia National Labs [23]. The recommended kinetic values for char oxidation reported by Hurt [24] $A = e^{8.12-0.0715(C,\%-daf)}$ $kg/(m^2 \cdot s \cdot atm_{O_2}^{0.5})$ for PRB coal and $E = 83.6$ kJ/mol were found to be within the desired accuracy by performing a linear sensitivity analysis. The results of the optimization were found not to be sensitive to product ratio parameters. The recommended values of Campbell [25], $A_{CO-CO_2} = 251$ and $E_{CO-CO_2} = 41.9$ kJ/mol, were found to be within the accuracy of the optimized parameters.

The char gasification kinetic parameters were subsequently optimized using these recommended parameters for char oxidation and product ratio. In addition, in the case of PRB coal feeding at 5 cm above the burner, two temperature measurements were excluded because it is believed that the temperature measurements are biased by the presence of volatile combustion. An example of the comparison among different simulation results and experimental data is shown in Figure 10. The optimized kinetic parameters for char gasification with carbon dioxide are $A_{CO_2} = 1200$ $kg/(m^2 \cdot s \cdot atm_{CO_2})$ and $E = 155$ kJ/mol. The optimized values for gasification with water vapor is $A_{H_2O} = 173$ $kg/(m^2 \cdot s \cdot atm_{H_2O})$ and $E = 457$ kJ/mol. The optimized value for the activation energy for gasification with water vapor is higher than values reported by others. Future tests at different temperatures and for different ranks of coals would allow further improvement in the optimized gasification parameters.

Conclusions

In this study, we investigated the effects of high concentrations of CO_2 and/or H_2O, on char burnout. We compared the total and elemental mass releases of the PRB sub-bituminous coal and its derived char under air-firing, cold-recycle and warm-recycle oxy-firing conditions at various residence times. As an important supplement to the mass release data, we also used an optical fiber based, two-color pyrometer to measure the single particle surface temperature and average particle velocity. The complete set of data revealed the difference in char burnout under these different firing conditions.

The results demonstrate that CO_2 and H_2O, present at relatively high levels under oxy-firing conditions, can have two major effects on char burnout through the gasification reactions. The gasification reactions can enhance burnout through the direct consumption of char. On the other hand, the endothermic nature of these reactions can lower the particle surface temperature and hence, decrease the char oxidation rate, which can in turn lead to lower char burnout. The dominance of either effect is dependent on the firing conditions (oxy vs. air, gas temperature) and coal type. In this study, cold-recycle oxy-firing increases char burnout over that of air-firing, indicating that mass removal by gasification with CO_2 dominates. In contrast, warm-recycle oxy-firing produces similar char burnout to that of air-firing, indicating comparable results through the two aforementioned effects. An improved char burnout model is needed to capture these effects, and predict the dominance of either effect under other firing conditions (temperature, oxygen level, etc.).

The modeling study carried out in this work is aimed to optimize the char gasification reaction rate parameters based on the experimental data using the existing model structure.
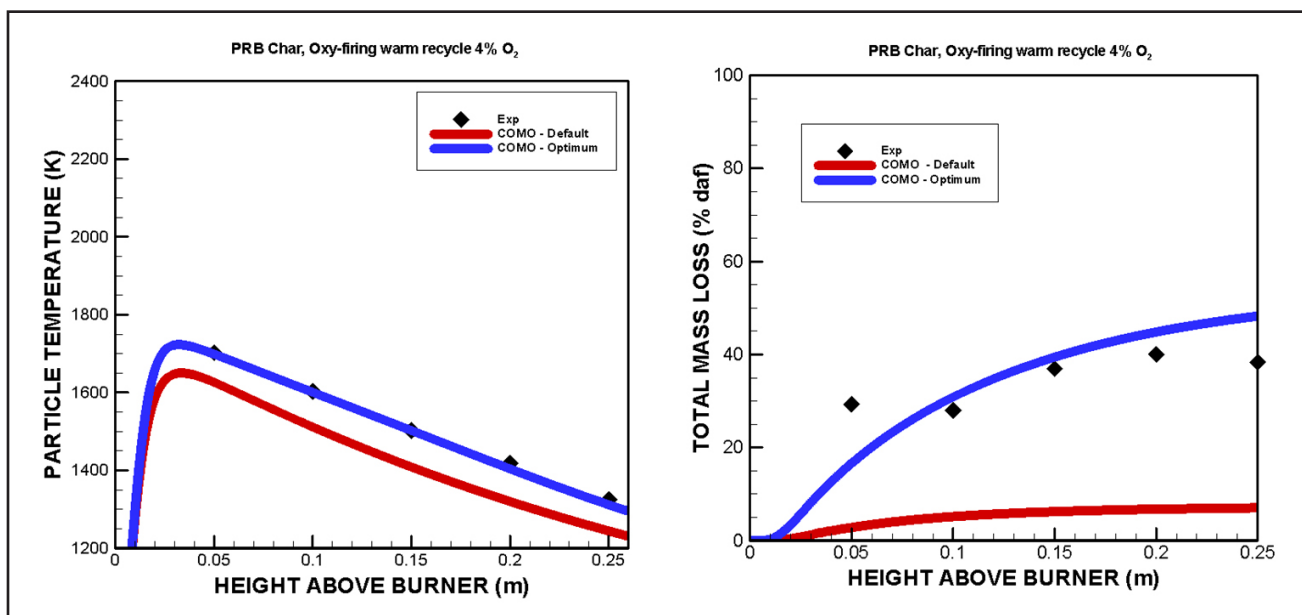

Fig. 10 Comparison of simulation and experimental results of particle mass loss and surface temperature (oxy-firing warm recycle, PRB char, 1500 °C, 4% O_2).

Significant improvement is made in the predictive ability of Field's char oxidation sub-model. It is recommended that half-order kinetics be used with the relationships recommended by Hurt [24] for all application of the char combustion in combination with values recommended by Campbell [25] for the product ratio parameters. Further measurements at different temperatures and mixtures of carbon dioxide and water vapor would allow improvement in the optimized gasification parameters.

References

1. R. M. Davidson and S. O. Santos, Oxyfuel Combustion of Pulverised Coal, IEA Clean Coal Centre, ISBN 978-92-9029-488-7, 2010.

2. B. J. P. Buhre, L. K. Elliott, C. D. Sheng, R. P. Gupta, and T. F. Wall, Oxy-Fuel Combustion Technology for Coal-Fired Power Generation. Progress in Energy and Combustion Science, 2005. 31: p. 283-307.

3. C. R. Shaddix and J. J. Murphy, Coal Char Combustion Reactivity in Oxy-Fuel Applications, in American Flame Research Committee International Symposium. 2003: Livermore, CA, USA.

4. C. R. Shaddix and J. J. Murphy, Coal Char Combustion Reactivity in O2/CO2 Recycle Applications, in Joint International Combustion Symposium. 2001: Kauai, USA.

5. C. R. Shaddix and A. Molina, Effect of O2 and High CO2 Concentrations on PC Char Burning Rates During Oxy-Fuel Combustion, in Proceedings of the 33rd International Technical Conference on Coal Utilization & Fuel Systems, The Clearwater Coal Conference. 2008: Sheraton Sand Key Clearwater, Florida, USA.

6. A. Molina and C. R. Shaddix. Ignition and Devolatilization of Pulverized Bituminous Coal Particles During Oxygen/Carbon Dioxide Coal Combustion in Proceedings of the Combustion Institute. 2007.

7. C. R. Shaddix and A. Molina. Particle Imaging of Ignition and Devolatilization of Pulverized Coal During Oxy-Fuel Combustion in Proceedings of the Combustion Institute. 2009.

8. L. Elliott, Y. Liu, B. Buhre, J. Martin, R. Gupta, and T. Wall, An Experimental and Mathematical Modeling Study Comparing the Reactivity and Burnout of Pulverized Coal in Air (O2/N2) and Oxyfuel (O2/CO2) Environments, in ICCS&T. 2005: Okinawa.

9. R. K. Rathnam, L. Elliott, B. Moghtaderi, R. Gupta, and T. Wall, Differences in Coal Reactivity in Air and Oxy-Fuel Conditions and Implications for Coal Burnout, in The Clearwater Coal Conference: The 31st International Technical Conference on Coal Utilization & Fuel Systems, Coal Technology: Whats Next? 2006: Clearwater, Fl.

10. R. K. Rathnam, T. F. Wall, K. Eriksson, L. Stromberg, and B. Moghtaderi, Reactivity of Pulverised Coals in Simulated Air (O2/N2) and Oxy-Fuel (O2/CO2) Atmospheres, in The 25th Annual International Pittsburgh Coal Conference. 2008: Pittsburgh, PA, USA.

11. S. Hu, D. Zeng, A. J. Mackrory, A. N. Sayre, and H. Sarv, Effects of CO2 on Char Oxidation and Ignition During Oxy-Coal Combustion, in 26th International Pittsburgh Coal Conference. 2009: Pittsburgh, PA.

12. P. A. Bejarano and Y. A. Levendis, Single-Coal-Particle Combustion in O2/N2 and O2/CO2 Environments. Combustion and Flame, 2008. 153: p. 270-287.

13. D. A. Tichenor, R. E. Mitchell, K. R. Hencken, and S. Niksa. Simultaneous in Situ Measurement of the Size, Temperature and Velocity of Particles in a Combustion Environment. in 20th Symposium (International) on Combustion. 1984.

14. W. J. Frederick, M. Hupa, J. Stenberg, and R. Hernberg, Optical Pyrometric Measurement of Surface Temperature During Black Liquor Char Burning and Gasification. Fuel, 1994. 73(12): p. 1889-1893.

15. J. Stenberg, W. J. Frederick, S. Boström, R. Hernberg, and M. Hupa, Pyrometric Temperature Measurement Method and Apparatus for Measuring Particle Temperatures in Hot Furnaces: Application to Reacting Black Liquor. Review of Scientific Instruments, 1996. 67(5): p. 1976-1984.

16. T. Joutsenoja, J. Stenberg, R. Hernberg, and M. Aho, Pyrometric Measurement of the Temperature and Size of Individual Combusting Fuel Particles. Applied Optics, 1997. 36(7): p. 1525-1535.

17. T. Joutsenoja and R. Hernberg, Pyrometric Sizing of High-Temperature Particles in Flow Reactors. Applied Optics, 1998. 37(16): p. 3487-3493.

18. T. Laurila, R. Oikari, T. Joutsenoja, P. Mikkola, T. Ranki-Kilpinen, P. Taskinen, and R. Hernberg, Pyrometric Temperature and Size Measurements of Chalcopyrite Particles During Flash Oxidation in a Laminar Flow Reactor. Metallurgical and Materials Transactions B - Process Metallurgy and Materials Processing Science, 2005. 36(2): p. 201-208.

19. J. Ma, Soot Formation and Secondary Reactions During Coal Pyrolysis. Doctor of Philosophy, Brigham Young University, 1996.

20. T. H. Fletcher, A. R. Kerstein, R. J. Pugmire, M. Solum, and D. M. Grant, A Chemical Percolation Model for Coal Devolatilization - Milestone Report, Sandia National Laboratories, SAND92-8207, 1992.

21. M. A. Field, D. W. Gill, B. B. Morgan, and P. G. W. Hawksley, Combustion of Pulverised Coal. 1967, Banbury, England: Cheney & Sons Ltd.

22. B. Raphael and I. F. C. Smith, A Direct Stochastic Algorithm for Global Search. Applied Mathematics and Computation, 2003. 146(2-3): p. 729-758.

23. R. E. Mitchell, R. H. Hurt, L. L. Baxter, and D. R. Hardesty, Compilation of Sandia Coal Char Combustion Data and Kinetic Analyses: Milestone Report, Sandia National Labs, SAND92-8208, 1992.

24. R. H. Hurt, J.-K. Sun, and M. Lunden, A Kinetic Model of Carbon Burnout in Pulverized Coal Combustion. Combustion and Flame, 1998. 113: p. 181-197.

25. P. A. Campbell, Investigation into the Roles of Surface Oxide Complexes and Their Distributions in the Carbon-Oxygen Heterogeneous Reaction Mechanism. Ph.D. Thesis, Stanford University, 2005.

Disclaimer

Although the information presented in this work is believed to be reliable, this work is published with the understanding that Babcock & Wilcox Power Generation Group and the authors are supplying general information and are not attempting to render or provide engineering or professional services. Neither Babcock & Wilcox Power Generation Group nor any of its employees make any warranty, guarantee, or representation, whether expressed or implied, with respect to the accuracy, completeness or usefulness of any information, product, process or apparatus discussed in this work; and neither Babcock & Wilcox Power Generation Group nor any of its employees shall be liable for any losses or damages with respect to or resulting from the use of, or the inability to use, any information, product, process or apparatus discussed in this work.